JOURNAL OF CATALYSIS 123, 456–462 (1990)

Encapsulation of Molecular Hydrogen in Zeolites at 1 atm

ANGELOS M. EFSTATHIOU,* STEVEN L. SUIB,*,†,[1] AND CARROLL O. BENNETT*

*Department of Chemical Engineering and †Department of Chemistry, University of Connecticut, Storrs, Connecticut 06268

Received June 20, 1989; revised January 2, 1990

About 1 μmol/g of molecular H_2 is encapsulated in the sodalite cages of NaX zeolite at 37°C and 1 bar H_2 pressure. The removal of this hydrogen by diffusion can be studied by temperature programming between 40 and 150°C under 1 bar Ar gas. The activation energy for diffusion is 8.1 kcal/mol. The amount of H_2 trapped is more than an order of magnitude less than that expected for chemisorption on a catalyst like cobalt on NaX. Exchanging Cs^+, Ni^{2+}, and Eu^{3+} for Na^+ cations into the supercages, hexagonal prisms, and sodalite cages, respectively, of X zeolite, leads to the conclusion that H_2 is trapped in the sodalite cages.

INTRODUCTION

In the course of characterization of some reduced metal-loaded NaX zeolite catalysts by H_2 chemisorption, we have noted a peak at about 85°C in the temperature programmed desorption (TPD) spectrum after adsorption of H_2 at 1 bar and room temperature. The results of this paper will show that about 1 μmol H_2/g is encapsulated at 1 bar and 37°C, compared to about 500 μmol/g at 88 bar and 300°C (*1*). We shall show that these small quantities can be measured precisely and that the form of the results indicates that the H_2 is actually trapped and not adsorbed on impurities. Part of the argument will be based on the change in quantity encapsulated as Na^+ is partially exchanged by Cs^+, Ni^{2+}, or Eu^{3+}, which are known to be concentrated respectively in the supercages, the hexagonal prisms, and the sodalite cages of X-type zeolite (*2*).

An early incentive for the study of H_2 encapsulation was the development of a means of storage for H_2 at high density without resort to high storage pressure (*1*, *3*). To our knowledge, this phenomenon has not been studied previously at atmospheric pressure nor for X-type zeolites.

EXPERIMENTAL

Preparation of zeolites. Linde NaX zeolite (600 mesh) was purchased from Alfa Ventron Corp. (Danvers, MA) and used without further purification. This material was ion-exchanged by taking 1 g of zeolite and stirring this for 18 h in a round-bottom flask with 0.05 *M* solutions of various cations. $Eu(NO_3)_3 \cdot 6H_2O$, $CsNO_3 \cdot 6H_2O$, and $Ni(NO_3)_2 \cdot 6H_2O$ salts purchased from Alfa Ventron were used for these solutions. Samples were filtered, washed with distilled deionized water, and dried under vacuum as previously described (*4*). The approximate formulas of the exchanged zeolites are $Eu_{25}Na_{11}X$, $Cs_{52}Na_{34}X$, and $Ni_{28}Na_{30}X$.

All zeolite samples were extensively dehydrated under vacuum prior to adsorption experiments. Samples were dehydrated at 50°C intervals for periods of about 1 h from 50 to 400°C on a vacuum line, evacuated to 5×10^{-6} Torr, sealed off and brought into a drybox, and loaded into a catalytic reactor. For TPD experiments, 0.2- to 1.2-g powdered samples were used, after compaction to 2 bar.

Characterization of zeolites. The degree of ion exchange in various zeolites has been studied with energy dispersive X-ray analy-

---

[1] To whom correspondence should be addressed.

0021-9517/90 $3.00

sis, atomic absorption, and neutron activation procedures (5). The crystallinity of the samples after ion exchange and after TPD studies was examined with X-ray powder diffraction (XRD) methods using a Phillips X-ray powder diffractometer with a Diano interface for control of scan speed, intensity, and time constant. Samples were loaded onto Vaseline-coated glass slides as previously described (6). XRD results for the ion-exchanged, calcined, and treated (after adsorption and TPD experiments) zeolites show that the samples all retained their structures with no loss of crystallinity.

Reactor-flow system. A once-through stainless-steel microreactor of 3.0 ml internal nominal volume described previously (7) was used in this study. To avoid air exposure of the catalyst during transfer and installation in the flow-panel, two-way valves were connected in the inlet and outlet leads of the reactor, which was loaded in a glovebox. Response experiments (7) have shown that the reactor behaves as an ideal mixed-flow reactor (CSTR) under the conditions used here: 0.55 g zeolite, 0.5 ml/s flow rate (ambient), and 2.3 ml gas-phase reactor volume.

Mass spectrometry. The high-resolution MS (Nuclide 12-90-G) produced flat-topped peaks for all the mass numbers studied. Sensitivity and background of components were recorded before and after each run. Results were obtained with a MINC-11 microcomputer (DEC) from an electron multiplier/electrometer ($\tau = 0.1$ s). Data acquisition and calibration were performed at the same acquisition frequency. To improve on the statistical noise and to have a high signal-to-noise ratio, 200 pts were collected at a frequency of 1 kHz and the average value was stored. Integration of the mass spectrometer response, expressed as concentration (ppm, mol%) vs time (min), was done by using the trapezoidal rule. The detection limit for H_2 was about 5 ppm. The ion source was operated at 70 eV electron acceleration potential. Hydrogen, H_2O, and Ar were recorded at $m/e = 2$, 18, and 40, respectively. The contribution of H_2O to the mass number 2 (H_2^+) ion signal was less than 0.5%.

RESULTS

Quantities of H_2 Encapsulation

Sorption and desorption of H_2 in dehydrated NaX. Before the initiation of sorption/desorption experiments, samples were checked *in situ* for residual water by MS. After the response of water (if present) at 400°C reached baseline, the reactor was closed off and cooled to the sorption temperature before the sorption/desorption experiments.

Figure 1 presents the results obtained with 1.1 g of dehydrated Na*X* when sorption occurred at 37°C with 1 bar H_2 and for the indicated period of time. The desorption was performed under 1 bar Ar and 15°C/min heating rate. Before the initiation of any TPD run, the reactor gas-phase volume was purged with Ar for 180 s at 37°C to ensure the complete removal of gas-phase H_2. At 37°C (zero time) some H_2 encapsulated in the zeolite diffused away from the surface and was measured. The rate of diffusion increased as temperature increased, and a maximum rate occurred between 78 and 92°C. The latter depended on the initial amount of hydrogen encapsulated in the ze-

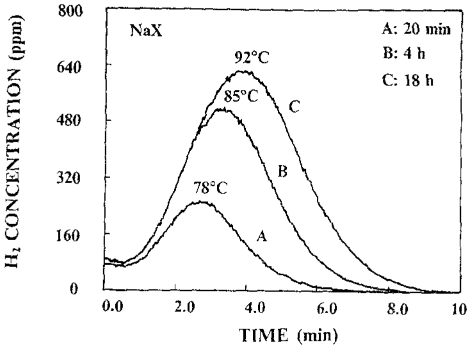

FIG. 1. TPD experiment for measuring H_2 encapsulated into Na*X*. Experimental procedure: H_2 (1 bar, 37°C, Δt) $\rightarrow$ Ar (180 s), 37°C $\rightarrow$ TPD (β = 15°C/min). Amount of sample used 1.1 g, flow rate 30 ml/min (ambient).

olite. A sorption time of 24 h produced only about a 5% increase in the H_2 uptake from that after 18 h in 1 bar H_2. This increase is within the accuracy of the analysis. Therefore, the H_2 uptake after 18 h under the conditions of the experiment represents the equilibrium amount established between the states of H_2 encapsulated in the zeolite cavities and that in the gas phase.

The effect of sorption temperature on the rate and amount of H_2 encapsulation for Na*X* is illustrated in Fig. 2. By increasing the temperature a notable increase in the uptake rate is noted, and for adsorption temperatures above 100°C the approach to the corresponding equilibrium value is very rapid. Within the first 20 min of adsorption, more than 90% of the equilibrium value is achieved. The curve for 18 h of exposure to H_2 at 1 bar is about equivalent to the equilibrium isobar at 1 bar.

Sorption and desorption of H_2 in ion-exchanged X zeolites. In order to probe the encapsulation site of H_2 in the zeolites, exchange with Cs^+, Eu^{3+}, and Ni^{2+} cations has been done, and the same sorption/desorption experiments as those with Na*X* were repeated by using 0.55-g samples. TPD results for Cs/Na*X* and Ni/Na*X* are shown in Fig. 3, and summarized in Fig. 4 and Table 1. There is zero H_2 uptake by Eu/Na*X* and a decrease in uptake for Cs/Na*X* and Ni/Na*X* with respect to Na*X*.

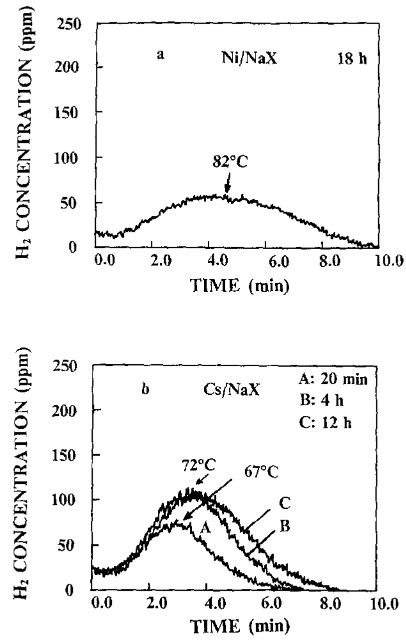

FIG. 3. TPD runs after various adsorption times. (a) Ni/Na*X*, (b) Cs/Na*X*. Experimental procedure: H_2 (1 bar, 37°C, Δt) → Ar (180 s), 37°C → TPD (β = 10°C/min). Amount of sample used 0.55 g.

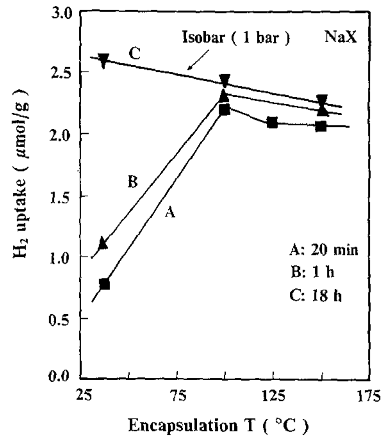

FIG. 2. Effect of temperature on the H_2 encapsulation amount for the Na*X* zeolite. Experimental procedure: H_2 (1 bar, *T*, Δt) → reactor closed off, cooled to 37°C → Ar (180 s), 37°C → TPD (β = 10°C/min).

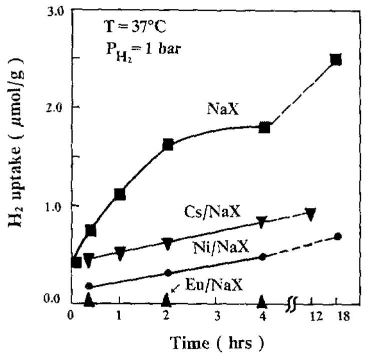

FIG. 4. Diffusion uptake of H_2 by various ion-exchanged Na*X* zeolites. The amount of H_2 encapsulation was determined according to the sequence: H_2 (1 bar, 37°C, Δt) → Ar (180 s), 37°C → TPD (β = 10°C/min).

TABLE 1

Hydrogen Uptake vs Time for Some Na*X* Zeolites (T = 37°C, P_{H_2} = 1 bar)

	H_2 uptake (μmol/g)			
Time	Na*X*	Cs/Na*X*	Ni/Na*X*	Eu/Na*X*
3 min	0.44	[a]	[a]	[a]
20 min	0.78	0.45	0.20	[b]
1 h	1.13	0.55	[a]	[a]
2 h	1.64	0.61	0.35	[b]
4 h	1.81	0.87	0.48	[b]
12 h	[a]	0.98	[a]	[a]
18 h	2.56	[a]	0.69	[a]
24 h	2.71	[a]	[a]	[a]

[a] Not measured.

[b] Zero H_2 uptake.

Rates of Encapsulation and Decapsulation

The curves in Fig. 4 can now be interpreted to obtain the diffusion parameters which control the encapsulation at 37°C and 1 bar H_2 pressure.

The classical solution of the diffusion problem for a sphere at constant temperature and subjected to a constant gas concentration starting at time zero is as follows (*8–10*):

$$\frac{Q(t) - Q(0)}{Q(\infty) - Q(0)} = 1 - \frac{6}{\pi^2} \sum_{n=1}^{\infty} \frac{1}{n^2} \exp\left(- \frac{D}{\alpha^2} \pi^2 n^2 t\right). \quad (1)$$

For small values of t

$$\frac{Q(t) - Q(0)}{Q(\infty) - Q(0)} = 6 \left(\frac{D}{\pi \alpha^2}\right)^{1/2} t^{1/2} \quad (2)$$

and for large values of t

$$\ln \left\{\frac{Q(\infty) - Q(t)}{Q(\infty) - Q(0)}\right\} = \ln \left(\frac{6}{\pi^2}\right) - \frac{D \pi^2 t}{\alpha^2}, \quad (3)$$

where Q represents the amount of adsorbate present in the zeolite crystallites at the indicated times and α is the radius of the spherical crystallite. Because of the assumptions made in deriving the diffusion equation, no attempt is made here to examine other crystallite geometries.

Figure 5 presents the results obtained after using Eqs. (2) and (3) to calculate the H_2 diffusivity (D/α^2) from sorption studies. For the case of Na*X* and for short times ($t \leq$ 45 min), a very good fit according to Eq. (2) is obtained. The quantity $Q(0)$ appearing in Eq. (2) was set equal to zero and that of $Q(\infty)$ equal to the corresponding equilibrium value under the experimental conditions used. For $t \geq$ 1 h, a deviation from Eq. (2) is observed and this is shown in Fig. 5. A value of $D/\alpha^2 = 5.5 \times 10^{-6}\ s^{-1}$ is obtained by Eq. (2), compared to $2.9 \times 10^{-6}\ s^{-1}$ obtained by Eq. (3). This difference is reasonable and might be related to assumptions made for constancy of the diffusivity. As equilibrium is approached, the dependence of the sorption curve on particle shape becomes significant, requiring a detailed knowledge (*8*) of particle shape when using Eq. (3). For Cs/Na*X* the value of D/α^2 is $1.3 \times 10^{-6}\ s^{-1}$.

From the TPD spectra of Figs. 1 and 3 it is possible to calculate diffusivities from the decapsulation process. The variation of D with temperature is given by

$$D(t) = D_0 \exp\left\{\frac{-E}{RT(t)}\right\}. \quad (4)$$

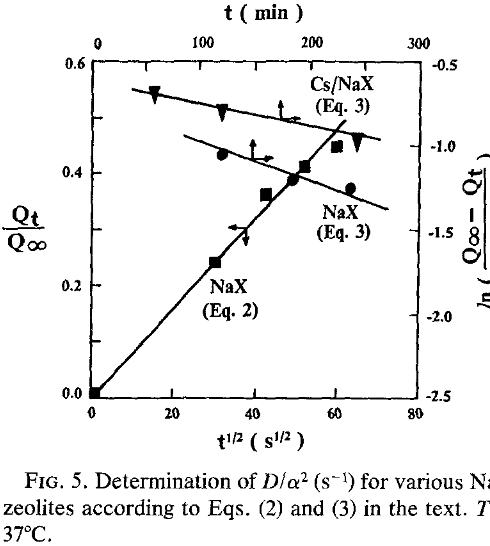

FIG. 5. Determination of D/α^2 (s^{-1}) for various Na*X* zeolites according to Eqs. (2) and (3) in the text. T = 37°C.

A detailed analysis for this case has been presented (*11, 12*), where peak shape and graphical methods can be used to calculate D_0 and E. The graphical method has been applied here, given by the following equation (*11, 12*):

$$\ln\left(\frac{T_M^2}{\beta}\right) = \frac{E}{RT_M} + \ln\left\{\frac{E\alpha^2}{1.5\,\pi^2 RD_0}\right\}. \quad (5)$$

By varying the heating rate β, the peak maximum temperature T_M is expected to vary, and by plotting the left-hand side of Eq. (5) against $1/T_M$ a straight line is expected. From this plot, E and D_0 can be calculated. Equation (5) has been applied to TPD spectra for Na*X* like those of Fig. 1, with encapsulation at 1 bar and 37°C for 20 min. The heating rate β is varied in the range 10–25 K/min, and it is found that $E = 8.1$ kcal/mol and $D_0/\alpha^2 = 50.1\ s^{-1}$. Then the use of Eq. (4) gives $D/\alpha^2 = 1.02 \times 10^{-4}\ s^{-1}$ at 37°C. This value is larger than that of about 3 to $5 \times 10^{-6}\ s^{-1}$ found from Fig. 5. Such behavior has been reported previously (*8*).

Blank experiments. Doubling the amount of Na*X* zeolite led to a doubling of H_2 sorption. This result excludes the possibility of any H_2 dissolution in the stainless-steel of the reactor under the conditions of the experiments. In addition, the Eu*X* experiments (Fig. 4) should give H_2 desorption from the steel, if the latter was indeed present. The possibility that H_2 sorption measurements could result from water (cracking effect) was also carefully examined. A small amount of water in the H_2 sorbate gas that is not removed by the traps might be present. For large times on stream, this water could accumulate in the zeolite and might contribute to the measured H_2^+ ion signal. Therefore, a separate H_2O TPD experiment with dehydrated Na*X* was performed, after the sample was treated with 1 bar H_2 for 18 h at 37°C. No H_2O signal was observed with MS between 37 and 350°C.

DISCUSSION

Hydrogen Encapsulation

It is appropriate to note that the TPD curves of Fig. 1 are not consistent with the chemisorption behavior of H_2 on metallic impurities. Experiments on Rh/Al_2O_3 show that T_M decreases with increasing amount of adsorbed H_2 present at the beginning of the TPD (*13*). This type of behavior has also been discussed by Balkenende *et al.* (*14*) and is consistent with the decrease in heat of adsorption as surface coverage increases. In Fig. 1 the opposite behavior appears. This result is consistent with decapsulation, which is controlled by diffusion rather than desorption from metallic sites.

Hydrogen sorption at 150°C for 18 h from a 30% H_2/70% Ar mixture at 1 bar produced a H_2 uptake only 15% of that obtained under the same conditions with pure H_2. This behavior is also not consistent with chemisorption, which is relatively insensitive to H_2 partial pressure. Rather, it corresponds to the encapsulation behavior already mentioned (*1*).

Figure 4 shows that all H_2 uptake is eliminated when Na^+ is largely exchanged with Eu^{3+}. This exchange would not be expected to result in zero uptake if the uptake were the result of some process other than encapsulation, such as adsorption on impurities, spillover, or sorption on the steel walls of the microreactor.

The signal-to-noise ratio of the data is good, and it is interesting that it is quite easy to measure encapsulation at 1 bar when the phenomenon has previously been studied only at pressures like 100–1000 bar. At full uptake at 37°C and 1 bar (Fig. 2), it is found that 0.035 molecules of H_2/unit cell are present, based on the data reported (Ref. (*19*), Table II) for Na*X*. This number represents a small fraction only of the available empty space in the cages, but the encapsulation seems to behave qualitatively as it does at the higher pressures.

Effect of Ion Exchange on Encapsulation

Again the results of the experiments with Eu/Na*X* are crucial to our arguments. We propose that $4Eu^{3+}$ ions are formed at the I′ sites in the sodalite cages, coordinated with an O^{2-} ion at the U site. The bulky Eu_4O^{+10} complex then prevents all encapsulation in the sodalite cages. The Eu^{3+} state in dehydrated *A* and *Y* zeolites has been confirmed (*15*). The apparent volume of the ions is not sufficient to explain the complete exclusion of H_2 trapping, so that it is probable that the strong fields set up by the multivalent cations play a role.

Considering now Na*X* and Cs/Na*X* zeolites, these ions are not expected to be complexed. The Cs^+ ions occupy the III sites and also the II sites near the 6-T rings but in the supercage (*2, 16*). In the presence of these ions the 12-T windows between the supercages are not blocked. However, the 6-T rings are partly obstructed, so that hydrogen which has entered the sodalite cages must cross an activation barrier in order to diffuse out when the external H_2 pressure is removed. The peak maximum temperature found in the TPD spectra for the Na*X* and the Cs/Na*X* (Figs. 1 and 3) are close to each other, so that there seems to be no great difference in the effective window space. Then the smaller encapsulation found for the Cs^+-exchanged zeolite with respect to Na*X* can be explained by the larger size of the Cs^+ ions.

Most of the Ni^{2+} ions in the Ni/Na*X* go to the I sites inside the hexagonal prisms and to the I′ sites in the sodalite cages (*2, 17*). The ions inside the hexagonal prisms may not affect encapsulation, but the replacement of some of the Na^+ by Ni^{2+} in the I′ sites may hinder passage through the 6-T rings into the sodalite cages, probably because of the higher electrostatic fields associated with the Ni^{2+}. Note that T_M for Ni/Na*X* is higher than those for Na*X* and Cs/Na*X*.

Clearly H_2 encapsulation is sensitive to the positions and charges of the ions in a zeolite structure. By studying the effect of the extent of exchange, the size and charge of the ion, and the size of the inert, nonpolar gas on encapsulation, a better understanding of the locations and effects of the ions can be obtained. The methods presented here should facilitate this task.

When zeolites are loaded with zero-valent metals to make catalysts, it is important and often difficult to know whether the metal clusters are inside or outside the crystals of zeolite. Suppression of encapsulation could be a probe showing that the clusters are inside.

Diffusion in Zeolites

It should be evident that the values of *D* appearing in the text refer to an effective diffusivity. Hydrogen should diffuse freely through the macropores between the zeolite crystals which make up the powder used. Passage through the supercages of the *X*-zeolite, connected by 12-T rings, is also relatively easy, so that the observed extremely slow uptake by diffusion is controlled by entry into the sodalite cages. Even the faster decapsulation process is still relatively slow, for the replacement of one gas by another in a typical pellet of silica or alumina is complete in a few seconds. It is interesting to note that for the Eu/Na*X* case, at the end of the 180 s of Ar purge at 37°C, before the TPD, no H_2 is obtained. This indicates that outward diffusion of hydrogen contained in the supercages and macropores during sorption is fast relative to the diffusion out of the sodalite cages.

Since the radius of the powder particles is thus irrelevant, α is unknown, and only (D/α^2) is reported. The actual mechanism for diffusion through the 6-T windows is unknown. Although wall effects are clearly important, Knudsen diffusion does not apply; the spaces are so small that the counterdiffusing molecules must collide. All this is complicated by the intracrystalline electrostatic fields. It is hardly surprising that (D/α^2) from Fig. 5 does not agree with that obtained from TPD spectra. Probably the best hope of understanding the process is through a Monte Carlo simulation (*18*).

CONCLUSIONS

The diffusion of molecular H_2 into Na*X* zeolite under atmospheric conditions, similar to those encountered in chemisorption studies, is slow near room temperature, where about 18 h is required to achieve an equilibrium state. When the temperature of adsorption increases above 100°C, an adsorption time of about 20 min brings the system very close to equilibrium. Molecular H_2 is finally encapsulated in the sodalite cages, where it can be expelled between 45 and 150°C with an activation energy of about 8.1 kcal/mol. The amount of H_2 encapsulation is no more than 5% of the H_2 that might be expected from a typical metal/Na*X* chemisorption system. Diffusivities of molecular H_2 were estimated under conditions similar to those encountered in catalytic studies. Hydrogen encapsulation in ion-exchanged zeolites may be considered as a sensitive method to probe the location of metal ions and particles in various sites of the zeolite.

ACKNOWLEDGMENTS

Support of this work was provided by the Department of Energy, Office of Basic Energy Sciences, Division of Chemical Sciences. Helpful discussions with Professor M. A. Vannice are gratefully acknowledged.

REFERENCES

1. Fraenkel, D., and Shabtai, J., *J. Amer. Chem. Soc.* **99,** 7074 (1977).
2. Smith, J. V., *in* "Zeolite Chemistry and Catalysis" (J. Rabo, Ed.), Vol. 171, p. 3–78. ACS Monograph, 1976.
3. Sesny, W. J., and Shaffer, L. H., US Patent 3 316 691, 1967.
4. Morrison, T. I., Reis, A. H., Gebert, E., Iton, L. E., Stucky, G. D., and Suib, S. L., *J. Chem. Phys.* **72,** 6276–6282 (1980).
5. Stucky, G. D., Iton, L. E., Morrison, T. I., Shenoy, G., Suib, S. L., and Zerger, R. P., *J. Mol. Catal.* **27,** 71–80 (1984).
6. Suib, S. L., McMahon, K. C., Tau, L. M., and Bennett, C. O., *J. Catal.* **89,** 20–34 (1984).
7. Stockwell, D. M., Chung, J. S., and Bennett, C. O., *J. Catal.* **112,** 135 (1988).
8. Eberly P. E., Jr, *in* "Zeolite Chemistry and Catalysis" (J. Rabo, Ed.), Vol. 171, pp. 392–436. ACS Monograph, 1976.
9. Crank, J., "The Mathematics of Diffusion." Clarendon Press, Oxford, 1956.
10. Aharoni, C., *Adsorp. Sci. Technol.* **1,** 1–29 (1984).
11. Fraenkel, D., *J. Chem. Soc. Faraday Trans. 1* **77,** 2029–2039 (1981).
12. Fraenkel, D., and Levy, A., *J. Chem. Soc. Faraday Trans. 1* **84**(6), 1817–1834 (1988).
13. Efstathiou, A. M., and Bennett, C. O., *J. Catal.*, accepted for publication (1990).
14. Balkenende, A. R., Geus, J. W., Kock, A. J. H. M., and Van der Pas, R. J., *J. Catal.* **115,** 365 (1989).
15. Suib, S. L., Zerger, R. P., Stucky, G. D., Morrison, T. I., and Shenoy, G. D., *J. Chem. Phys.* **80,** 2203–2207 (1984).
16. Hseu, K., PhD thesis, University of Washington (1973).
17. Gallezot, P., and Imelik, B., *J. Phys. Chem.* **77,** 652 (1973).
18. Aust, E., Dahlke, K., and Emig, G., *J. Catal.* **115,** 86–97 (1989).
19. Breck, D. W., and Grose, R. W., *Adv. Chem. Ser.* **121,** 322 (1973).